

# A Constrained Motion Approach to the Synchronization of Multiple Coupled Slave Gyroscopes

Harshavardhan Mylapilli<sup>1</sup>

<sup>1</sup>*Department of Aerospace and Mechanical Engineering  
University of Southern California  
Los Angeles, California 90089, USA  
[mylapill@usc.edu](mailto:mylapill@usc.edu)*

**Abstract -** A set of ‘n’ gyroscopes are coupled together to form a system of ‘slave’ gyroscopes. A simple approach is developed for synchronizing the motion of these slave gyroscopes, whose individual motion may be regular or chaotic, with the motion of an independent ‘master’ gyroscope irrespective of the chaotic or regular motion exhibited by the master. The problem of synchronization of these multiple gyroscopes is approached from a constrained motion perspective through the application of the Udwadia-Kalaba equation. The approach yields explicit, closed form expressions for the control torques that are required to be applied to each of the coupled slave gyroscopes and achieves ‘exact’ synchronization with the master’s motion. The influence of different types of interactions between the slave gyroscopes is investigated through the use of an incidence matrix which describes the coupling between any two of them. The effect of the so-called ‘sleeping’ condition on the synchronization of the gyroscopes is also explored. To illustrate the efficacy of the methods presented in this paper, we consider numerical examples involving systems of multiple gyroscopes and synchronize them with the motion of a master gyroscope.

**Keywords –** Multiple Gyroscopes; Udwadia-Kalaba Equation; Synchronization; Constrained Motion; Nonlinear control; Chain coupled systems; General coupled systems

## Introduction

Gyroscopes have long been used in navigation due to their ability to measure orientation. From aerospace vehicles to consumer electronic devices, gyroscopes have played an important role in our everyday lives. From an engineering point of view, gyroscopes are highly nonlinear mechanical systems that exhibit a plethora of complicated motions such as periodic behavior, period-doubling behavior, quasi-periodic behavior and chaotic behavior. Studies (Tong and Mrad 2001; Ge and Chen 1996a,b; Van Dooren 2003) have shown that when a symmetric gyroscope with linear plus cubic damping is subjected to a harmonic vertical base excitation, the motion thus obtained can range from regular motion to chaotic motion depending on the parameters selected.

In analytical mechanics, the problem of synchronization of multiple chaotic systems has been of particular interest in recent times (Leipnik and Newton 1981; Pecora and Carroll 1990). In particular, the problem of synchronizing a set of ‘slave’ gyroscopes which may or may not be coupled to each other, to an independent master gyroscope is an important problem in nonlinear dynamics that has received considerable attention (Chen 2002; Lei and Xu 2005; Udwadia 2008). This problem gains prominence in the field of spacecraft dynamics where attitude control of spacecraft is almost always performed using gyroscopes. When there are multiple gyroscopes onboard a spacecraft, it is often required that they be synchronized to indicate a specific, usable spacecraft pointing. And given that these gyroscopes exhibit a wide range of dynamic behavior, the problem of synchronization becomes even more challenging. The synchronization problem also finds applications in areas of secure communication (e.g. transmission of encrypted messages) and in areas of signal processing (Strogatz 2000). A large number of papers written on

this subject only seem to consider the synchronization problem of two *identical* gyroscopes. Chen (2002) considers two *identical* chaotic gyros with different initial conditions and uses numerous classical control laws to show that when the feedback gain (obtained through experimentation) exceeds a particular value, the slave gyro synchronizes with the master gyro. Lei and Xu (2005) approach the same problem using feedback linearization wherein the difference in response between the master and slave gyro is taken as an error signal and a time varying control is chosen to drive the error signal to zero. Aghababa (2011), on the other hand, considers an adaptive robust finite-time controller to synchronize two chaotic gyros inspite of unknown uncertainties in the system. These approaches to the synchronization of master/slave gyros appear to work when the number of slaves considered is small in number. However, when a large number of slaves with *non-identical* physical and geometric properties are considered, the need to develop efficient control methods arise. It is also important to note that many papers on this subject assume that the gyroscopes are in the so-called ‘sleeping position’, which in general is an over-simplifying condition, since most gyroscopes do not satisfy it.

Recently, Udwadia and Han (2008) approached the problem of synchronization of multiple chaotic gyroscopes from a new perspective - using the constrained motion approach. In their paper, Udwadia and Han consider a system of ‘n’ gyroscopes, each in the so-called ‘sleeping’ position, which are all uncoupled from one another having varying physical and geometrical properties, some or all of which exhibiting chaotic behavior, and attempt to synchronize these uncoupled slave gyros with a master gyro. The problem of synchronization, which is classically considered as a tracking control problem in control theory, is recast as a problem of constrained motion. The slaves are suitably constrained and the Udwadia-Kalaba equation is used in arriving at the nonlinear control torques that force exact synchronization of each slave gyro with the

master gyro. However, the problem with synchronizing a master gyro with ‘n’ *uncoupled* slave gyroscopes is that it can effectively be simplified into ‘n’ separate problems of synchronization of the master gyro with ‘n’ individual slave gyros.

In this paper, we consider a set of ‘n’ *coupled* gyros such that they form a single system of interacting slave gyroscopes. Next, we attempt to synchronize this nonlinear system of slave gyros with an independent master gyroscope whose motion can be either regular or chaotic. We adopt the methods developed by Udwadia and Han (2008) and build on them to derive the constrained equations of motion for the case when the slave gyroscopes are all coupled. In the process, we also obtain explicit and closed form expressions for the generalized nonlinear control torques that are required to be applied to each of the slave gyros to obtain synchronization with the master gyro. We consider both linear and highly nonlinear types of coupling (that include linear plus cubic coupling, sinusoidal coupling and Toda coupling (Toda 1981)) between the slave gyroscopes. The effect of the ‘sleeping’ condition on the synchronization of the gyros is also studied. Further, utilizing the concept of an incidence matrix, we also examine the case when the slave gyroscopes are coupled in a more general fashion (instead of the usual chain coupling). Finally, to illustrate the efficacy of the methods presented in this paper, we provide three numerical simulations. We consider a system of five gyros with one master and four chain coupled slaves where the slaves are coupled (a) using sinusoidal coupling (b) using Toda coupling. In the Toda coupling case, the effect of the no-sleeping condition on the synchronization of the gyros is studied. The third example consists of a system of six gyroscopes with one master and five slaves where the slaves are coupled to one another through an incidence matrix with different types of strongly nonlinear couplings.

## Equations of Motion

Consider the system of ‘n+1’ symmetric gyroscopes as shown in Figs. 1-2. The master gyro whose parameters are denoted by the subscript ‘m’ is an independent system separate from the slave gyroscopes. The other ‘n’ gyroscopes (denoted by subscripts 1 to n) are all coupled together with torsion springs to form the system of slave gyros. In the present study, we use Euler angles to describe the orientation of each gyroscope – ‘ $\theta$ ’ (nutation), ‘ $\varphi$ ’ (precession) and ‘ $\psi$ ’ (spin).

**Master Gyroscope** - The nonlinear equation of motion of a symmetric gyroscope whose point of support  $O$  is subjected to a vertical harmonic excitation of frequency  $\omega_m$  and amplitude  $\tilde{d}_m$  has been derived by Udwadia and Han (2008) and is reproduced below:

$$I_m \ddot{\theta}_m + \frac{(p_{\varphi_m} - p_{\psi_m} \cos \theta_m)(p_{\psi_m} - p_{\varphi_m} \cos \theta_m)}{I_m \sin^3 \theta_m} - m_m g r_m \sin \theta_m - m_m r_m \sin \theta_m \ddot{d}_m(t) = F_d, \quad (1)$$

where the angular momenta  $p_{\psi_m} = I_{3_m}(\dot{\psi}_m + \dot{\phi}_m \cos \theta_m)$  and  $p_{\varphi_m} = I_m \dot{\phi}_m \sin^2 \theta_m + p_{\psi_m} \cos \theta_m$  are conserved quantities since  $\psi_m$ ,  $\varphi_m$  happen to be cyclic co-ordinates,  $m_m$  denotes the mass of the master gyroscope,  $I_m = I_{1_m} + m_m r_m^2$  where  $I_{1_m} = I_{2_m}$  denote the principal equatorial moment of inertia of the master gyroscope whereas  $I_{3_m}$  denotes the polar moment of inertia,  $\theta_m$ ,  $\psi_m$ ,  $\varphi_m$  are the Euler angles of rotation associated with the master gyroscope,  $r_m$  denotes the distance along the polar axis of the center of mass of the gyro from its point of support (see figure 1) and  $d_m(t) = \tilde{d}_m \sin(\omega_m t)$  is the time-varying amplitude of the vertical support motion that has frequency  $\omega_m$ . The non-conservative damping force acting on the master gyroscope  $F_d = -\bar{c}_m \dot{\theta}_m - \bar{e}_m \dot{\theta}_m^3$  is assumed to be of linear plus cubic type (Ge et al. 1996). A stationary symmetric gyro positioned with its axis along the vertical usually falls over. However, when it is given a sufficiently large

spin about the vertical axis, it begins to rotate in a stable fashion, with its axis remaining very close to the vertical. The symmetric gyro showing this type of ‘sleeping top’ motion is said to be in a ‘sleeping position’ and this usually happens when the angular momenta ( $p_\psi = p_\phi = p$ ) is constant for all time  $t$ . The equation of motion of the vertically excited master gyro (1) in the ‘sleeping position’ is then given by

$$\underbrace{\ddot{\theta}_m + \alpha_m^2 \frac{(1-\cos\theta_m)^2}{\sin^3\theta_m} + c_m \dot{\theta}_m + e_m \dot{\theta}_m^3 - \beta_m \sin\theta_m + \gamma_m \sin\theta_m \sin(\omega_m t)}_{-F_m^{gyro}} = 0, \quad (2)$$

where  $P_m = \left\{ \alpha_m = \frac{p_m}{I_m}, \beta_m = \frac{m_m g r_m}{I_m}, c_m = \frac{\tilde{c}_m}{I_m}, e_m = \frac{\tilde{e}_m}{I_m}, \gamma_m = \frac{m_m r_m \tilde{d}_m \omega_m^2}{I_m}, \omega_m, I_m \right\}$  is the parameter set that describes the physical characteristics of the master gyroscope.

**Slave Gyroscopes** - Consider the system of ‘n’ symmetric gyroscopes which are coupled in chain fashion as shown in Figure 2. The subscript  $i$  (where  $i = 1$  to  $n$ ) denotes each individual slave gyroscope. Each of the slave gyros is subjected to a vertical harmonic base excitation of amplitude  $\tilde{d}_i$  and frequency  $\omega_i$ . The slaves are also subjected to a non-conservative damping force which is of linear plus cubic type related only to the  $\theta$  coordinate. The following types of torsion spring couplings are studied in the present paper –

1. Harmonic coupling

$$V_i^t(\theta_{i+1} - \theta_i) = \sigma_i (1 - \cos(\theta_{i+1} - \theta_i)), \quad (3)$$

2. Toda torsion coupling (Toda 1981)

$$V_i^t(\theta_{i+1} - \theta_i) = \frac{a_i}{b_i} e^{b_i(\theta_{i+1} - \theta_i)} - a_i(\theta_{i+1} - \theta_i) - \frac{a_i}{b_i}, \quad (4)$$

3. Linear plus cubic coupling

$$V_i^t(\theta_{i+1} - \theta_i) = \frac{f_i}{2} (\theta_{i+1} - \theta_i)^2 + \frac{g_i}{4} (\theta_{i+1} - \theta_i)^4 \quad (5)$$

where  $a_i$ ,  $b_i$ ,  $f_i$ ,  $g_i$ ,  $\sigma_i$  are the spring constants corresponding to the  $i^{\text{th}}$  spring element and  $V'_i$  denotes the torsional potential energy of the  $i^{\text{th}}$  spring element in the chain.

Consider the  $i^{\text{th}}$  gyroscope in the slave system. Besides the forces  $F_i^{\text{gyro}}$  (see equation 6) that act on a symmetric gyro as a consequence of it being subjected to nonlinear damping and vertical excitation, the only additional forces that act on it are the coupling forces. Thus, the equation of motion of the  $i^{\text{th}}$  slave gyroscope in the  $\theta_i$  direction can be computed using Newton's laws as follows –

$$\ddot{\theta}_i + \underbrace{\frac{(p_{\varphi_i} - p_{\psi_i} \cos \theta_i)(p_{\psi_i} - p_{\varphi_i} \cos \theta_i)}{I_i^2 \sin^3 \theta_i} + \frac{\tilde{c}_i \dot{\theta}_i}{I_i} + \frac{\tilde{e}_i \dot{\theta}_i^3}{I_i} - \frac{m_i g r_i}{I_i} \sin \theta_i - \frac{m_i r_i}{I_i} \sin \theta_i \ddot{d}_i(t)}_{-F_i^{\text{gyro}}} = \frac{1}{I_i} \underbrace{\left( \frac{\partial V^T(\theta_{i+1} - \theta_i)}{\partial \theta_i} - \frac{\partial V^T(\theta_i - \theta_{i-1})}{\partial \theta_i} \right)}_{F_{i+1,i}^S - F_{i,i-1}^S} \quad (6)$$

where  $p_{\psi_i} = I_{3i}(\dot{\psi}_i + \dot{\phi}_i \cos \theta_i)$ ,  $p_{\varphi_i} = I_i \dot{\phi}_i \sin^2 \theta_i + p_{\psi_i} \cos \theta_i$ ,  $d_i(t) = \tilde{d}_i \sin(\omega_i t)$ ,  $F_{i+1,i}^{\text{sine}} = \sigma_i \sin(\theta_{i+1} - \theta_i)$  for a harmonic coupling,  $F_{i+1,i}^{\text{Toda}} = a_i [e^{b_i(\theta_{i+1} - \theta_i)} - 1]$  for a Toda coupling and  $F_{i+1,i}^{\text{LC}} = f_i(\theta_{i+1} - \theta_i) + g_i(\theta_{i+1} - \theta_i)^3$  for a linear plus cubic coupling. Since,  $\psi_i$  and  $\varphi_i$  are cyclic coordinates, equation (6) alone is sufficient to describe the equation of motion of the  $i^{\text{th}}$  slave gyro. Equation (6) can be represented more conveniently as

$$\ddot{\theta}_i = F_i^{\text{gyro}} + \frac{1}{I_i} (F_{i+1,i}^S - F_{i,i-1}^S) \quad (7)$$

where  $F_i^{\text{gyro}}$  are the gyroscopic forces acting on the  $i^{\text{th}}$  gyro due to it being subjected to vertical excitation and nonlinear damping and  $F_{i+1,i}^S$  is the coupling force exerted by the  $(i+1)^{\text{th}}$  gyro on the  $i^{\text{th}}$  gyro. In the present study, we approach the problem of synchronization of multiple gyroscopes from a constrained motion perspective, which includes three vital steps. The first step

involves the derivation of the equations of motion of the unconstrained system. The second step involves the formulation of the constraint equations and the last step deals with the use of Udwadia-Kalaba equation (Udwadia and Kalaba 1996a, b) to obtain the constrained equations of motion of synchronized master-slave system. In the process, we also find a closed form expression for the explicit nonlinear control torques that are required to be applied to each of the slave gyroscopes to synchronize them precisely with the motion of the master gyroscope.

**Unconstrained Equations of Motion** - In the present paper, the independent master gyroscope (1) along with the system of coupled slave gyroscopes (7) forms the unconstrained system (Udwadia and Kalaba 1996). The unconstrained equation of motion of the system can be written down in matrix form (using equation 2 and 6) as follows

$$M_{(n+1) \text{ by } (n+1)} \begin{bmatrix} \ddot{\theta}_m \\ \ddot{\theta}_1 \\ \vdots \\ \ddot{\theta}_i \\ \vdots \\ \ddot{\theta}_n \\ \ddot{x}_{n+1 \text{ by } 1} \end{bmatrix} = \begin{bmatrix} F_m^{\text{gyro}} + F_{2,1}^S/I_1 \\ F_1^{\text{gyro}} + (F_{i+1,i}^S - F_{i,i-1}^S)/I_i \\ \vdots \\ F_i^{\text{gyro}} + (-F_{n,n-1}^S)/I_n \\ \vdots \\ F_n^{\text{gyro}} \end{bmatrix}, \quad (8)$$

where  $M$  is an identity matrix of size ' $n+1$ '. The unconstrained acceleration of the system is given by  $\ddot{a} = M^{-1}F = F$ . To this unconstrained system, we impose a set of constraints such that the system of coupled slave gyros precisely follows the master gyroscope in its motion.

**Constraint Equations** - The unconstrained system (8) is subjected to the following set of constraints –

- 1] **No Control Force on the Master Gyro** – Since the motion of the master gyroscope is considered to be independent of the motion of the slave gyroscopes; the need to apply a control

force on the master gyro does not arise in the constrained system. Hence, the unconstrained motion of the master gyroscope can itself be considered as a constraint equation. Thus, we have

$$\ddot{\theta}_m = F_m^{gyro}. \quad (9)$$

**2] Synchronization Constraint -** In the present paper, our goal is to synchronize the motion of each of the coupled slave gyros with that of the master gyro. Hence, the following set of ‘n’ constraints are imposed on the unconstrained system and are given by

$$\nu_i = \theta_m - \theta_i = 0, \quad i=1, 2, 3 \dots n \quad (10)$$

However, it may be possible to initiate the slave gyros from positions in phase space that may not satisfy the constraints (10). This problem is surmounted by choosing appropriate trajectory stabilization parameters  $\delta, k$  (Udwadia 2003; 2008) such that

$$\ddot{\nu}_i + \delta \dot{\nu}_i + k \nu_i = 0 \Rightarrow \ddot{\theta}_m - \ddot{\theta}_i = -\delta(\dot{\theta}_m - \dot{\theta}_i) - k(\theta_m - \theta_i) \quad (11)$$

Thus, the unconstrained system (8) is subjected to a total of ‘ $n+1$ ’ cumulative constraints in order to achieve synchronization of each individual coupled slave gyro with the motion of the master gyro. When the constraints (9) and (11) are expressed in the constraint matrix form, we obtain

$$\begin{bmatrix} [1] & [0 & \cdots & 0] \\ [1] & [-I_{n \text{ by } n}] \\ \vdots \\ [1] \end{bmatrix}_{A_{n+1 \text{ by } n+1}} \begin{bmatrix} \ddot{\theta}_m \\ \ddot{\theta}_1 \\ \vdots \\ \ddot{\theta}_i \\ \vdots \\ \ddot{\theta}_n \end{bmatrix}_{\ddot{X}_{n+1 \text{ by } 1}} = \begin{bmatrix} F_m^{gyro} \\ -\delta(\dot{\theta}_m - \dot{\theta}_1) - k(\theta_m - \theta_1) \\ \vdots \\ -\delta(\dot{\theta}_m - \dot{\theta}_i) - k(\theta_m - \theta_i) \\ \vdots \\ -\delta(\dot{\theta}_m - \dot{\theta}_n) - k(\theta_m - \theta_n) \end{bmatrix}_{b_{n+1 \text{ by } 1}}. \quad (12)$$

**Constrained Equations of Motion -** With all the requisite matrices ( $M, F, A, b$ ) at our disposal, the constrained equations of motion can now be calculated using the Udwadia-Kalaba equation

(Udwadia and Kalaba 2002). Since,  $M = I_{n+1}$  and  $A$  is a square matrix of size ' $n+1$ ', the expression for the control force reduces to –

$$F^C = M^{\frac{1}{2}} \left( AM^{-\frac{1}{2}} \right)^+ (b - Aa) = A^+ (b - Aa) = A^{-1} (b - Aa) \quad (13)$$

The constraint matrix  $A$  is structured in such a way that it possesses the unique property:  $A^{-1} = A$  and this reduces the explicit expression of the nonlinear control torques to –

$$\begin{aligned} F^C &= A^{-1} (b - Aa) = A^{-1}b - A^{-1}Aa = Ab - a = \\ &= \begin{bmatrix} [1] & [0 \ \dots \ 0] \\ [1] & [-I_{n \text{ by } n}] \end{bmatrix} \begin{bmatrix} F_m^{gyro} \\ -\delta(\dot{\theta}_m - \dot{\theta}_1) - k(\theta_m - \theta_1) \\ \vdots \\ -\delta(\dot{\theta}_m - \dot{\theta}_i) - k(\theta_m - \theta_i) \\ \vdots \\ -\delta(\dot{\theta}_m - \dot{\theta}_n) - k(\theta_m - \theta_n) \end{bmatrix} - \begin{bmatrix} F_m^{gyro} \\ F_1^{gyro} + F_{2,1}^S/I_1 \\ \vdots \\ F_i^{gyro} + (F_{i+1,i}^S - F_{i,i-1}^S)/I_i \\ \vdots \\ F_n^{gyro} + (-F_{n,n-1}^S)/I_n \end{bmatrix} \\ &= \begin{bmatrix} 0 \\ \{\delta(\dot{\theta}_m - \dot{\theta}_1) + k(\theta_m - \theta_1)\} + F_m^{gyro} - \left( F_1^{gyro} + \frac{F_{2,1}^S}{I_1} \right) \\ \vdots \\ \{\delta(\dot{\theta}_m - \dot{\theta}_i) + k(\theta_m - \theta_i)\} + F_m^{gyro} - \left( F_i^{gyro} + \frac{F_{i+1,i}^S - F_{i,i-1}^S}{I_i} \right) \\ \vdots \\ \{\delta(\dot{\theta}_m - \dot{\theta}_n) + k(\theta_m - \theta_n)\} + F_m^{gyro} - \left( F_n^{gyro} + \frac{-F_{n,n-1}^S}{I_n} \right) \end{bmatrix} \quad (14) \end{aligned}$$

where  $\delta, k$  are the trajectory stabilization parameters and  $F^{gyro}, F^S$  are the gyroscopic forces and coupling forces respectively. Thus, equation (14) gives us the explicit, closed form expression for the nonlinear control torques (devoid of any approximations or simplifications) that needs to be applied to the unconstrained system to obtain the constrained system. The constrained equations of motion of the system are now given by (Udwadia and Kalaba 1996; 2002):

$$M \ddot{X} = F + F^C \quad (15)$$

where  $F$  is given by the RHS of equation (8) and  $F^C$  is given by the equation (14). This completes our derivation of the constrained system of equations (15) and they represent the governing equations of motion of the coupled slave gyroscopes which follow a ‘given’ master gyroscope (be it chaotic or regular).

**Incidence Matrix -** Until now, we have considered the case wherein the slave gyros are all coupled in a chain fashion. But it is indeed possible to consider a more general interaction wherein a particular slave gyro can be coupled to any number of other slave gyros without any restrictions. Now, in such a case, it becomes imperative to keep track of the coupling information between any two slave gyros in the system. This can be succinctly done by the use of the incidence matrix. The incidence matrix has the following salient features –

- The incidence matrix, denoted by  $\xi$ , is a symmetric matrix of size ‘n’ (where ‘n’ denotes the number of slave gyros). It gives us information about the coupling between any two slave gyroscopes in the system.
- Each element of the incidence matrix  $\xi$  is restricted to have a value of either 0 or 1. A zero value of  $\xi_{ij}$  indicates that the  $i^{th}$  and  $j^{th}$  slaves are uncoupled whereas a unitary value of  $\xi_{ij}$  indicates that the  $i^{th}$  slave is coupled to the  $j^{th}$  slave.
- Since a gyroscope cannot be coupled to itself, the diagonal elements of the incidence matrix are all zero (i.e.  $\xi_{ii} = 0$ ;  $i = 1, 2, 3 \dots n$ ).

Thus, given an incidence matrix that describes the various different interactions between a set of coupled slave gyros, the unconstrained equations of motion of the  $i^{th}$  slave gyro in the system can be written down as follows

$$\ddot{\theta}_i = F_i^{gyro} + \frac{1}{I_i} \left( \sum_{\substack{j=1 \\ j \neq i}}^n \xi_{ij} F_{ij}^{Couple} \right), \quad i = 1, 2, 3 \dots n, \quad (16)$$

where  $F_{ij}^{Couple} = -F_{ji}^{Couple}$ . This set of ‘n’ equations along with the unconstrained motion of the independent master gyro (equation 2) forms the unconstrained system. The reader can now utilize the methods described in this section to re-derive the constrained equations of motion of the master-slave system and generate the necessary control torques that are required to be applied to the slave system of gyroscopes such that they synchronize precisely with the motion of the master gyroscope.

### Results and Simulations

To better illustrate the efficacy of the methods presented in this paper, we present three numerical simulations. In the first example, we consider a system of five gyros (1 Master + 4 Slaves) with the sleeping condition imposed on all five gyros. We examine the effect of sinusoidally chain coupling the slave gyros on the synchronization of the gyros. In the second example, we consider a system of six gyros (1 Master + 5 Slaves) and use an incidence matrix to describe the various different interactions between the five coupled slave gyros. The sleeping condition is imposed on all six gyros and different types of linear and nonlinear couplings are used between the individual slaves. In the final example, we consider a five gyro system (1 Master + 4 Slaves) and explore the effect of the ‘sleeping condition’ on the synchronization of the gyros.

Throughout this paper, the integration of the equations of motion (constrained as well as unconstrained) is performed using the MATLAB ODE45 scheme with a relative error tolerance of 10e-9 and an absolute error tolerance of 10e-12. Further, the Lyapunov exponents for the master-slave system of gyroscopes are computed using the methods described in (Udwadia and Von Bremmen 2000; 2001; 2002) over a time span of 1000 seconds. To determine these exponents,

integration has been performed, once again, using the MATLAB ODE45 scheme with a relative error tolerance of 10e-9 and an absolute error tolerance of 10e-13.

### Synchronization with the use of a Sleeping Condition

#### a. Five gyroscopes (1 Master + 4 Coupled Slaves) using a Sine coupling

Consider a system of five non-identical gyroscopes (1 Master + 4 Slaves) where the set of four slave gyroscopes are all connected in a chain fashion using a sinusoidal coupling (described by equation 3) with coefficients  $\sigma_{12} = 2$ ,  $\sigma_{23} = 1.5$ ,  $\sigma_{34} = 2.5$ . All gyros are assumed to be in the ‘sleeping’ position and we have  $p_{\varphi_i} = p_{\psi_i} = p_i$ ,  $i = m, 1, 2, 3, 4$ . Each individual slave gyro (although coupled to other slaves) is required to precisely track the motion of the master gyro. Table 1 gives the parameter sets  $P_i = \{\alpha_i, \beta_i, c_i, e_i, \gamma_i, \omega_i, I_i\}$ ,  $i = m, 1, 2, 3, 4$  that describe the characteristics of each of the gyros of the master-slave system and their initial condition sets  $IC_i = [\theta_i^0, \dot{\theta}_i^0, \tau_i^0]$ . Using the parameters in Table 1, the Lyapunov exponents for the master gyroscope and the system of slave gyroes are computed to be  $l_m = \{-0.179707, -0.500232, 0\}$  and  $l_s = \{0.121455, 0.066865, 0.004824, -0.039699, -0.253232, 0.000107, -0.568669, -0.645423, 0.000110, -0.728986, -0.777867, 0\}$  respectively. Since the values of  $l_m$  are either negative or zero, the master gyro is said to exhibit regular periodic motion. The slave system on the other hand appears to be chaotic.

The unconstrained system consists of the master gyroscope and the set of four coupled slave gyroscopes whose equations of motion can be written down using equations (8). Figure 3 shows a phase plot  $(\theta_m, \dot{\theta}_m)$  of the unconstrained motion of the master gyroscope. Clearly, the motion of the master is periodic as also indicated by its Lyapunov exponents. Figure 4, on the other hand,

shows a phase plot  $(\theta_i, \dot{\theta}_i)$ ,  $i=1,2,3,4$  of the unconstrained motion of the individual slave gyroscopes. The phase plots (Figs. 3-4) are all plotted in the time range  $150 \leq t \leq 200$  seconds. A superimposed image of the time history of the nutation angle  $\theta$  of the five gyros is plotted in Figure 5 showing that prior to synchronization, the five gyros exhibit highly nonlinear behavior and their trajectories vary widely from each other.

To this unconstrained system, we impose a set of five constraints (as described by equation (12) with trajectory stabilization constants  $\delta=1$  and  $k=2$ ) and compute the constrained equations of motion using equation (15). A superimposed phase plot of the constrained motion of the master-slave system of gyros is plotted in Figure 6 for  $150 \leq t \leq 200$ . As can be seen from the figure, the four slave gyros with sinusoidal chain coupling between them synchronize precisely with the periodic motion of the master gyroscope. Figure 7 shows the time history of nutation angle  $\theta$  post synchronization; the control forces take less than 10 seconds to exponentially reduce the error between the motion of master and the individual slaves to zero. Figure 8 shows a time history of synchronization errors for  $60 \leq t \leq 200$ . Note that the error converges exponentially as demanded by equation (11). The synchronization errors are of the order of  $10e-13$  which is lesser than the tolerance levels used in MATLAB ODE45 integration scheme showing the efficacy of the control forces in achieving synchronization. Thus, a system of four non-identical slave gyroscopes which are sinusoidally chain coupled to each other have been shown to precisely track the motion of a master gyroscope exhibiting periodic motion.

### b. Six gyroscopes (1 Master + 5 Coupled Slaves) using the Incidence matrix

In the present example, we consider a system of six non-identical gyroscopes (1 Master + 5 Coupled Slaves) where the interaction between the five slaves is more general and is described

by an incidence matrix. The five coupled gyros are required to precisely track the motion of the independent master gyro (described by the parameter set  $P_m$ ), which in this case exhibits chaotic motion as seen from its Lyapunov exponents  $l_m = \{0.206668, -0.896620, 0\}$ . The coupling between the slaves (with parameter sets  $P_i, i = 1, 2, 3, 4, 5$  given in Table 2) is described by the 5-by-5 incidence matrix  $\xi$  as shown below-

$$\xi = \begin{bmatrix} 0 & 1_T & 0 & 1_L & 1_S \\ 1_T & 0 & 1_S & 0 & 1_L \\ 0 & 1_S & 0 & 1_{LC} & 0 \\ 1_L & 0 & 1_{LC} & 0 & 0 \\ 1_S & 1_L & 0 & 0 & 0 \end{bmatrix} \quad (17)$$

The interaction between the  $i^{\text{th}}$  and  $j^{\text{th}}$  slaves is characterized by the value of the  $(i, j)^{\text{th}}$  element of the matrix  $\xi$ . The subscripts  $L, S, T$  and  $LC$  of the  $(i, j)^{\text{th}}$  element of the incidence matrix denotes *Linear*, *Sinusoidal*, *Toda*, and *Linear + Cubic* couplings respectively. Figure 9 depicts a pictorial representation of the incidence matrix showing the various types of couplings used between the individual slave gyroscopes. The unconstrained equations of motion of the master (2) and the five coupled slave gyroscopes (16) which are all assumed to be in the ‘sleeping’ position can now be written down as

$$\ddot{\theta}_m = F_m^{\text{gyro}} \quad (18)$$

$$\ddot{\theta}_1 = F_1^{\text{gyro}} + \frac{1}{I_1} (F_{12}^{\text{Toda}} + F_{14}^{\text{Linear}} + F_{15}^{\text{Sine}}) \quad (19)$$

$$\ddot{\theta}_2 = F_2^{\text{gyro}} + \frac{1}{I_1} (F_{21}^{\text{Toda}} + F_{23}^{\text{Sine}} + F_{25}^{\text{Linear}}) \quad (20)$$

$$\ddot{\theta}_3 = F_3^{\text{gyro}} + \frac{1}{I_1} (F_{32}^{\text{Sine}} + F_{34}^{\text{Linear + Cubic}}) \quad (21)$$

$$\ddot{\theta}_4 = F_4^{\text{gyro}} + \frac{1}{I_1} (F_{41}^{\text{Linear}} + F_{43}^{\text{Linear + Cubic}}) \quad (22)$$

$$\ddot{\theta}_5 = F_5^{\text{gyro}} + \frac{1}{I_1} (F_{51}^{\text{Sine}} + F_{52}^{\text{Linear}}) \quad (23)$$

where  $F_i^{gyro}$  is given by (6),  $F_{ij}^{Toda} = a_{ij} \left[ e^{b_{ij}(\theta_j - \theta_i)} - 1 \right]$ ,  $F_{ij}^{\text{Sine}} = \sigma_{ij} \sin(\theta_j - \theta_i)$ ,  $F_{ij}^{\text{Linear}} = \lambda_{ij} (\theta_j - \theta_i)$ ,  $F_{ij}^{\text{Linear + Cubic}} = f_{ij}(\theta_j - \theta_i) + g_{ij}(\theta_j - \theta_i)^3$  and  $F_{ij}^{\text{Couple}} = -F_{ji}^{\text{Couple}}$   $\forall i < j$ ;  $i, j = 1, 2, 3, 4, 5$ . The spring constants are given by the following parameters:  $a_{12} = 1.5$ ,  $b_{12} = 0.05$ ,  $\lambda_{14} = 0.5$ ,  $\sigma_{15} = 2$ ,  $\sigma_{23} = 1.2$ ,  $\lambda_{25} = 0.3$ ,  $f_{34} = 0.8$ ,  $g_{34} = 0.04$ . Based on these parameters, the Lyapunov exponents for the system of slave gyros are calculated to be  $l_s = \{0.082678, 0.051033, 0.015758, -0.007526, -0.075204, 0.000197, -0.424779, -0.483015, 0.000402, -0.523197, -0.646143, 0.000002, -0.723966, -0.787581, 0\}$ . Based on these exponents, the slave system appears to be chaotic.

Figure 10 shows a phase plots of  $(\theta_i, \dot{\theta}_i), i = m, 1, 2, 3, 4, 5$  of the unconstrained system (18-23) for  $50 \leq t \leq 100$ . The master gyroscope exhibits chaotic motion as predicted by  $l_m$ . From figure 10, we can infer that all six gyros exhibit highly nonlinear behavior and are unsynchronized. The constrained (synchronized) equations of motion for this system of six gyros can once again be computed using equation (15) with the application of six constraints (see equation 12). The phase plots of the constrained system  $(\theta_i \text{ vs } \dot{\theta}_i), i = m, 1, 2, 3, 4, 5$  have been plotted in Figure 11 for  $50 \leq t \leq 100$  (left) and  $150 \leq t \leq 200$  (right), where we observe that the plot of each gyro has been superposed on top of another, indicating synchronization of the five slave gyros with the chaotic motion of the master. Figure 12 shows a time history of the nutation angle ‘ $\theta$ ’ for  $0 \leq t \leq 20$ . As can be inferred from the figure, it takes less than 10 seconds for the slave gyros to track the motion of the chaotic master gyro. Figure 13 shows a time history of the synchronization errors in ‘ $\theta$ ’ for each slave gyroscope in the time range of  $60 \leq t \leq 200$ . The vertical scale of the figure shows that the error is of the order of  $10e-13$  signifying that the errors in the simulation are within the tolerance levels of the ODE45 integration scheme. A time history of generalized control torques applied to each individual slave gyroscope to achieve synchronization with the

chaotic master gyro is shown in Figure 14. Thus, given a set of five non-identical general coupled slave gyros where the coupling between the gyros is prescribed by the incidence matrix, we managed to precisely synchronize the motion of the each of the slave gyros with that of the chaotic master gyro, something quite significant for chaotic systems since they show extremely sensitive dependence to initial conditions.

### Synchronization without the use of the Sleeping Condition

In this section, we attempt to synchronize a set of non-identical gyroscopes without using the so called ‘sleeping condition’ and show that synchronization can indeed be obtained even without the need to assume that the gyros are in ‘sleeping’ position. If we remove the simplification of a sleeping condition, then we no longer assume that  $p_{\varphi_i} = p_{\psi_i} = p_i$  and hence  $p_{\varphi_i}, p_{\psi_i}$  are chosen to be two different constants. Angular momenta  $p_{\varphi_i}, p_{\psi_i}$  are associated with cyclic coordinates  $\varphi_i, \psi_i$  respectively and are therefore constant and cannot change with time. The imposition of the ‘no sleeping’ condition brings in an additional two parameters  $p_{\varphi_i}, p_{\psi_i}$  into the dynamics of each individual gyroscope and they are appended at the end of the set  $P$  to give the new

$$\text{parameter set } P_i = \left\{ \alpha_i = \frac{1}{I_i}, \beta_i = \frac{m_i g r_i}{I_i}, c_i = \frac{\tilde{c}_i}{I_i}, e_i = \frac{\tilde{e}_i}{I_i}, \gamma_i = \frac{m_i r_i \tilde{d}_i \omega_i^2}{I_i}, \omega_i, p_{\varphi_i}, p_{\psi_i} \right\}.$$

#### a. Five gyroscopes (1 Master + 4 Coupled Slaves) using a Toda coupling

Consider a system of five non-identical gyroscopes (with parameter sets given by Table 3) where the set of four slave gyros are coupled in a chain fashion using a Toda torsion spring coupling. Each individual coupled slave gyro is required to exactly track the motion of the master gyro ( $l_m = \{-0.223403, -0.226832, 0\}$ ) which in this case exhibits regular periodic motion. The coefficients of the Toda spring elements are given by  $a_{12} = 1.20$ ;  $a_{23} = 1.50$ ;  $a_{34} = 1.25$ ;  $b_{12} =$

$0.11$ ;  $b_{23} = 0.13$ ;  $b_{34} = 0.105$ . The system of slave gyros appears to exhibit chaotic behavior as indicated by its Lyapunov exponent set given by  $l_s = \{0.107805, -0.015994, 0.000394, -0.121534, -0.634956, 0.000173, -1.390733, -1.850994, 0.000002, -1.881298, -1.976043, 0\}$ .

Since the simplification of the sleeping condition is removed, the unconstrained equations of motion of the master and the individual slave gyros are given by equations (1) and (6) respectively. A superimposed phase plot of the unconstrained motion of the periodic master gyroscope  $(\theta_m, \dot{\theta}_m)$  along with the unconstrained motion of each individual coupled slave gyros  $(\theta_i, \dot{\theta}_i)$ ,  $i=1,2,3,4$  is shown in Figure 15. The phase plots are all plotted in the time range  $50 \leq t \leq 100$ . The non-identical gyros exhibit highly nonlinear behavior as expected with their trajectories varying widely from each other. The constrained equations of motion of the master-slave system of gyroscopes are computed using equation (15) with the application of five constraints as described by (12). A superimposed phase plot of the constrained motion of the master-slave system of gyros is plotted in Figure 16 for  $50 \leq t \leq 100$ . As can be seen from the figure, the four slave gyros (which are all chain coupled) synchronize exactly with the periodic motion of the master gyroscope. The phase plot of each gyro has superposed on top of the other indicating precise synchronization with the master gyro. Figure 17 shows the time history of nutation angle  $\theta$  for the five gyros post synchronization. The control torques take less than 10 seconds to synchronize the motion of individual slaves with that of the periodic master gyroscope. Figure 18, on the other hand, shows the time history of synchronization errors for  $60 \leq t \leq 100$ . The exponential convergence of the errors to zero is evident. And finally, figure 19 shows a time history of the nonlinear control torques acting on the individual slave gyroscopes to obtain synchronization with the master gyro. Thus, we conclude that the removal of the ‘sleeping’ condition has had little effect on the synchronization of the master-slave system of gyros.

## Conclusions

In the present study, we consider the problem of synchronization of a system of ‘n’ chain-coupled or generally-coupled slave gyroscopes with that of a master gyroscope. However, this classical problem of tracking is approached from a constrained motion perspective. The tracking requirements are recast as constraints and the Udwadia-Kalaba equation is used to obtain the constrained (synchronized) equations of motion of the master-slave system of gyroscopes. In the process, explicit nonlinear control torques are calculated (in closed form) that are used to drive the system of coupled slave gyroscopes to synchronize exactly with the motion of the master gyroscope (irrespective of the chaotic or periodic behavior displayed by the master/slave system of gyroscopes).

1. Previous investigators concern themselves with the synchronization of a set of one or two uncoupled slave gyroscopes with the motion of a master gyroscope. But the theory developed in this paper allows for a set of ‘n’ slave gyroscopes which are all coupled to one another to synchronize with the motion of the master gyro. Each slave gyro is a highly nonlinear system; in addition the slaves are nonlinearly coupled to one another with different types of couplings and this leads to a highly nonlinear, complex dynamical system. However, the control torques are found with relative ease showing the power and efficacy of the underlying control methods.
2. The control torques derived in this paper are continuous in time and in theory lead to exact synchronization of the master-slave system of gyroscopes. No approximations have been made in the derivation of these non-linear control torques, or in approximating the highly nonlinear dynamics of either the master or any of the coupled slave gyroscopes.
3. The equations of motion of master-slave system of gyros are derived without applying the simplification of the sleeping condition. Although many authors on this subject assume the

gyros to be in sleeping position, in general however, most gyros do not satisfy this condition.

In this paper, it is shown that removal of the sleeping condition has little effect on the synchronization of the gyroscopes as is evident from numerical simulation.

4. To show the efficacy of the methods presented in this paper, numerical simulations involving multiple non-identical gyroscopes, with various types of couplings between the slave gyros, is presented. In all the cases, the control torques provided by the Udwadia-Kalaba equation leads to an exact synchronization of the master-slave system of gyros irrespective of the chaotic or regular motions exhibited by the individual gyroscopes. It should be noted that the methods presented in this paper are applicable to any number of slave gyroscopes and given any type of general, nonlinear coupling among them. The speed with which synchronization is achieved can be controlled by appropriately modifying the trajectory stabilization parameters.
5. The constrained motion approach and the Udwadia-Kalaba equation are powerful tools to obtain the equations of motion of constrained nonlinear mechanical systems. Thus, the methodologies provided in this paper can be readily adopted and expanded to synchronize other general nonlinear dynamical systems.

## References

1. Aghababa, M.P., A novel adaptive finite-time controller for synchronizing chaotic gyros with nonlinear inputs, *Chin. Phys. B* 20 (2011) 090505.
2. Chen, H.K., 2002, "Chaos and Chaos Synchronization of a Symmetric Gyro With Linear-Plus-Cubic Damping," *J. Sound Vib.*, 2554, pp. 719–740.
3. Ge, Z.M., and Chen, H.H., 1996, "Bifurcation and Chaos in Rate Gyro With Harmonic Excitation," *J. Sound Vib.*, 1941, pp. 107–117.
4. Ge, Z.M., Chen, H.K., and Chen, H.H., 1996, "The Regular and Chaotic Motions of a Symmetric Heavy Gyroscope With Harmonic Excitation," *J. Sound Vib.*, 1982, pp. 131–147.
5. Lei, Y., Xu, W., and Zheng, H., 2005, "Synchronization of Two Chaotic Nonlinear Gyros Using Active Control," *Phys. Lett. A*, 343, pp. 153–158.
6. Leipnik, R. B., and Newton, T. A., 1981, "Double Strange Attractors in Rigid Body Motion With Linear Feedback Control," *Phys. Lett.*, 86A, pp. 63–67.
7. Pecora, L.M., and Carroll, T.L., 1990, "Synchronization in Chaotic Systems," *Phys. Rev. Lett.*, 64, pp. 821–824.
8. Strogatz, S., 2000, *Nonlinear Dynamics and Chaos*, Westview, Cambridge, MA.
9. Toda M., *Theory of Nonlinear Lattices*, Springer-Verlag, Berlin, 1981.
10. Tong, X., and Mrad, N., 2001, "Chaotic Motion of a Symmetric Gyro Subjected to Harmonic Base Excitation," *ASME J. Appl. Mech.*, 68, pp. 681–684.
11. Udwadia F. E. and H. von Bremen, "A Note on the Computation of the Largest p-Lyapunov Characteristic Exponents for Nonlinear Dynamical Systems," *Applied Math. and Computation*, 114, pp. 205-214, 2000.
12. Udwadia F. E. and H. von Bremen, "An Efficient and Stable Approach for Computation of Lyapunov Characteristic Exponents of Continuous Dynamical Systems," *Applied Math. and Computation*, 121, pp. 219-259, 2001.

13. Udwadia F. E., and H. von Bremen, "Computation of Lyapunov Characteristic Exponents for Continuous Dynamical Systems," *Zeitschrift fur Angewandte Mathematik und Physik*, 53, pp.123-146, 2002.
14. Udwadia, F. E. and Kalaba, R. E., "What Is the General Form of the Explicit Equations of Motion for Constrained Mechanical Systems," *Journal of Applied Mechanics*, Vol. 69, No. 3, 2002, pp.335-339.
15. Udwadia, F. E., "A New Perspective on the Tracking Control of Nonlinear Structural and Mechanical Systems," *Proceedings of the Royal Society A*, Vol. 459, 2003, pp. 1783-1800.
16. Udwadia, F. E., "Nonideal Constraints and Lagrangian Dynamics," *Journal of Aerospace Engineering*, Vol.13, No.1, 2000, pp.17-22.
17. Udwadia, F. E., "Optimal Tracking Control of Nonlinear Dynamical Systems," *Proceedings of the Royal Society A*, Vol. 464, 2008, pp. 2341-2363.
18. Udwadia, F. E., and Kalaba, R. E., "Analytical Dynamics: A New Approach," Cambridge University Press, Cambridge, England, 1996.
19. Udwadia F. E. and R. E. Kalaba, "Equations of Motion for Mechanical Systems," *Journal of Aerospace Engineering*, 9, pp. 64-69, 1996.
20. Udwadia, F., Han, B., "Synchronization of Multiple Chaotic Gyroscopes Using the Fundamental Equation of Mechanics", *Journal of Applied Mechanics*, Vol. 75, 02011, 2008.
21. Van Dooren, R., "Comments on Chaos and Chaos Synchronization of a Symmetric Gyro With Linear-Plus-Cubic Damping," *J. Sound Vib.*, 268, pp. 632–634, 2003.

Journal of Aerospace Engineering. Submitted August 16, 2011; accepted December 14, 2011;  
posted ahead of print December 16, 2011. doi:10.1061/(ASCE)AS.1943-5525.0000192

### **List of Figure Captions**

Figure 1: Symmetrical master gyro (independent) subjected to vertical harmonic excitation.

Figure 2: A system of chain coupled slave gyroscopes. Each slave gyro in the chain is subjected to vertical harmonic excitation resulting, when uncoupled from the system, in regular or chaotic motion.

Figure 3: A phase plot of the unconstrained motion of the periodic master gyroscope for  $150 \leq t \leq 200$

Figure 4: A phase plot of the unconstrained motion of four slave gyroscopes which are all coupled to one another in a chain fashion ( $150 \leq t \leq 200$ ).

Figure 5: Time history of  $\theta$  for each individual gyroscope for  $0 \leq t \leq 20$  prior to synchronization

Figure 6: A superimposed phase plot of the constrained motion of five gyroscopes for  $150 \leq t \leq 200$ . The slave gyroscopes have precisely synchronized with the motion of the master gyro.

Figure 7: Time history of  $\theta$  for each individual gyroscope for  $0 \leq t \leq 20$  in the constrained system. Slave gyros take less than 10 seconds to synchronize with the motion of the master gyro

Figures 8: Time history of synchronization errors for  $60 \leq t \leq 200$ . Errors are smaller than the tolerance levels of the integration scheme.

Figure 9: General - Coupled Slave Gyroscope System depicting various types of coupling/interactions between the slaves.

Figure 10: A phase plot of the unconstrained motion for each individual gyroscope for  $50 \leq t \leq 100$ . The master gyroscope is independent whereas the other remaining five slave gyroscopes are all coupled using the incidence matrix.

Figure 11: A superimposed phase plot of the constrained motion of five gyroscopes for  $50 \leq t \leq 100$  (left) and  $150 \leq t \leq 200$  (right). Slave gyros have precisely tracked motion of the master gyro.

Figure 12: Time history of  $\theta$  for each individual gyroscope for  $0 \leq t \leq 20$  in the constrained system.

Figures 13: Time history of synchronization errors for  $60 \leq t \leq 200$  (bottom). Errors are smaller than the tolerance levels of the integration scheme.

Figure 14: Generalized control torques acting on each individual slave gyroscope for  $0 \leq t \leq 200$ .

Figure 15: Superimposed phase plot depicting the unconstrained motion of the periodic master gyro along with the four chain coupled slave gyros for  $50 \leq t \leq 100$ .

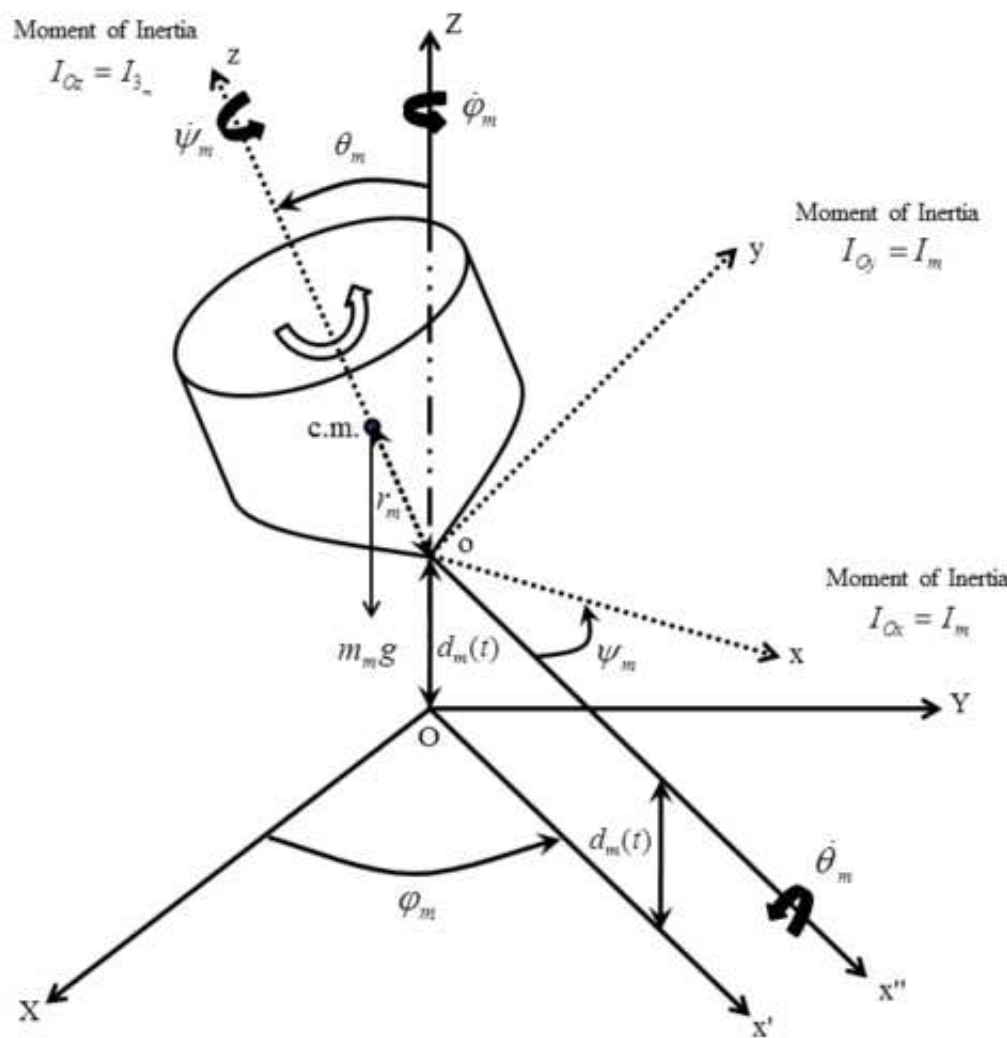
Figure 16: A superimposed phase plot of the constrained motion of five gyroscopes for  $50 \leq t \leq 100$ . The slave gyroscopes have precisely synchronized with the motion of the master gyro.

Figure 17: Time history of  $\theta$  for each individual gyroscope for  $0 \leq t \leq 20$  in the constrained system.

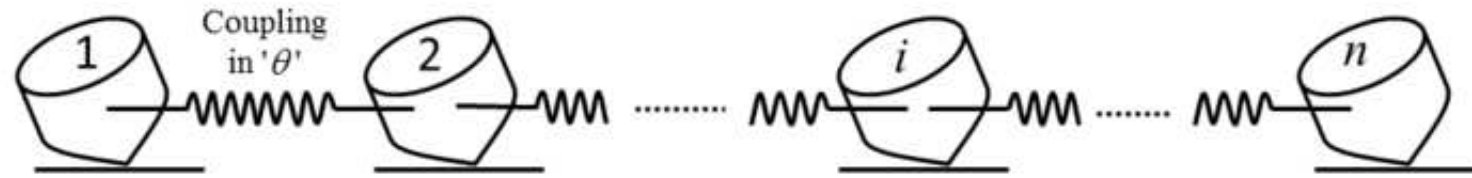
Figure 18: Time history of synchronization errors for  $60 \leq t \leq 100$ . Errors are smaller than the tolerance levels of the integration scheme.

Figure 19: Time history of the control torques acting on each individual slave gyroscope for  $0 \leq t \leq 100$ .

Accepted Manuscript  
Not Copyedited



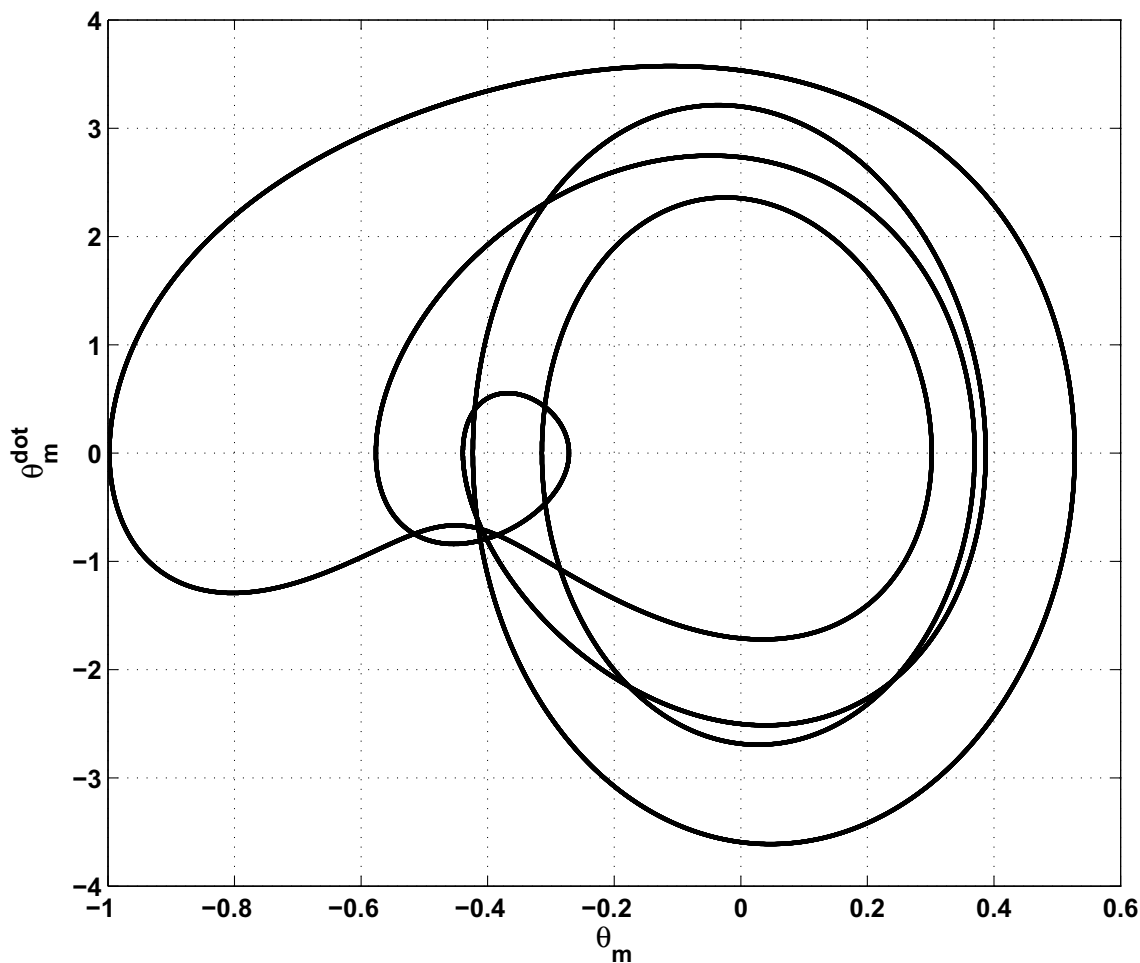
Journal of Aerospace Engineering. Submitted August 16, 2011; accepted December 14, 2011;  
posted ahead of print December 16, 2011. doi:10.1061/(ASCE)AS.1943-5525.0000192



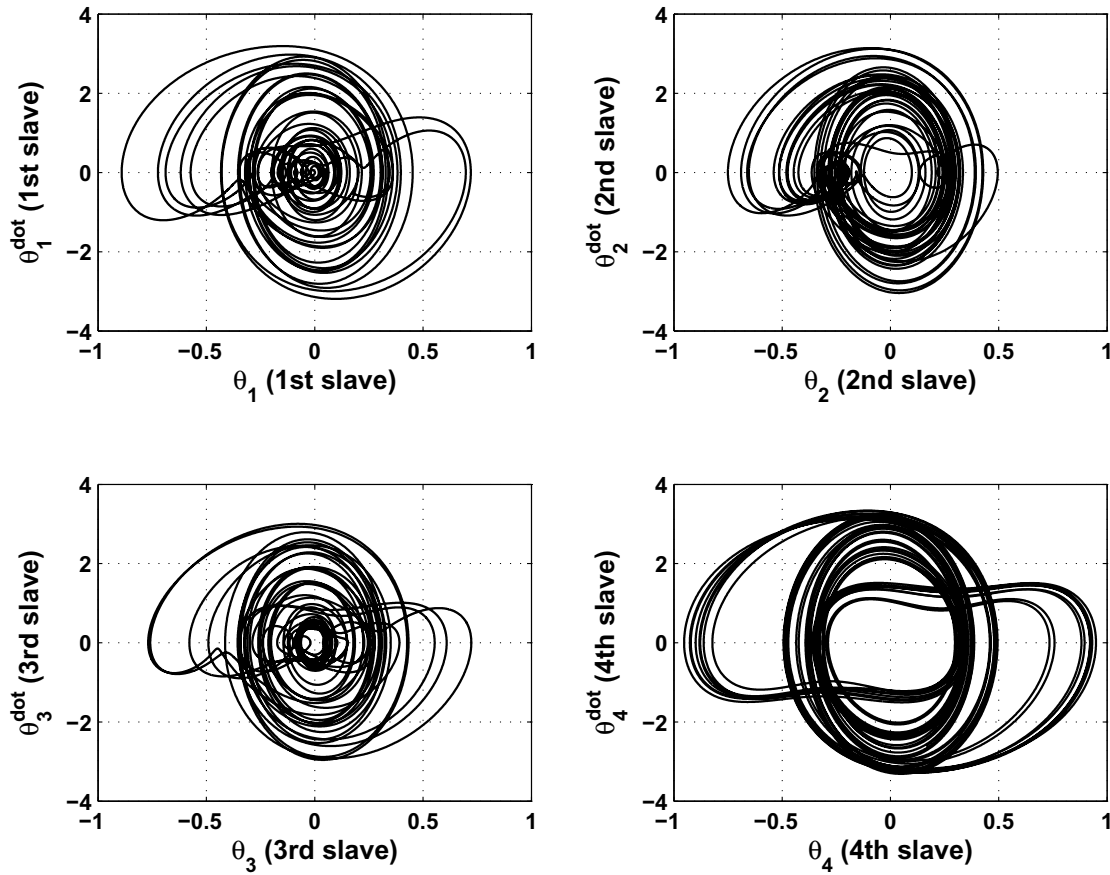
Accepted Manuscript  
Not Copyedited

Figure 3

Journal of Aerospace Engineering. Submitted August 16, 2011; accepted December 14, 2011;  
posted ahead of print December 16, 2011. doi:10.1061/(ASCE)AS.1943-5525.0000192



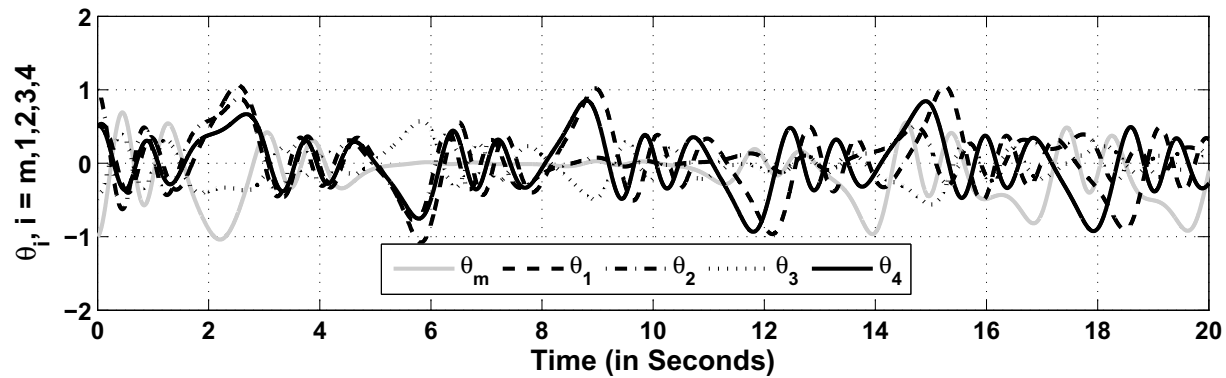
Accepted Manuscript  
Not Copyedited



Accepted Manuscript  
Not Copyedited

Figure 5

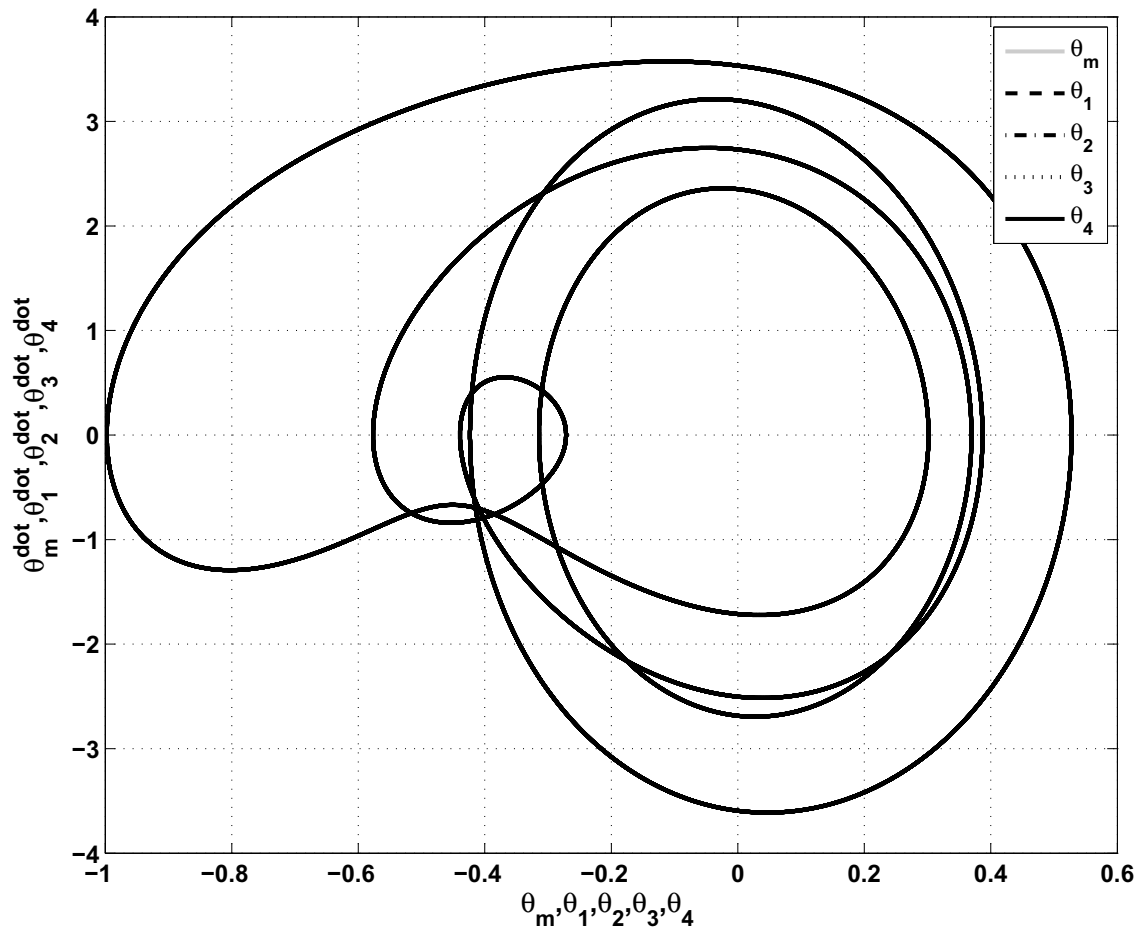
Journal of Aerospace Engineering. Submitted August 16, 2011; accepted December 14, 2011;  
posted ahead of print December 16, 2011. doi:10.1061/(ASCE)AS.1943-5525.0000192



Accepted Manuscript  
Not Copyedited

Figure 6

Journal of Aerospace Engineering. Submitted August 16, 2011; accepted December 14, 2011;  
posted ahead of print December 16, 2011. doi:10.1061/(ASCE)AS.1943-5525.0000192



Accepted Manuscript  
Not Copyedited

Figure 7

Journal of Aerospace Engineering. Submitted August 16, 2011; accepted December 14, 2011;  
posted ahead of print December 16, 2011. doi:10.1061/(ASCE)AS.1943-5525.0000192

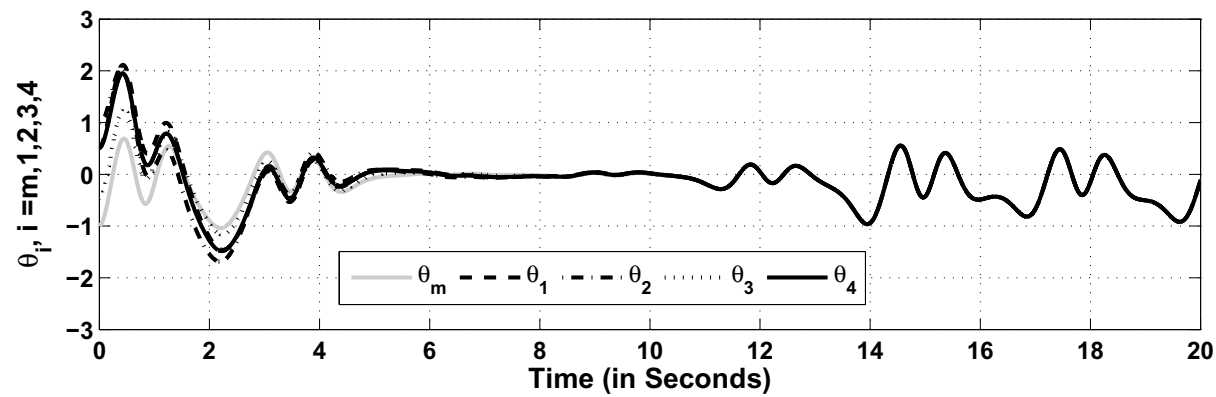
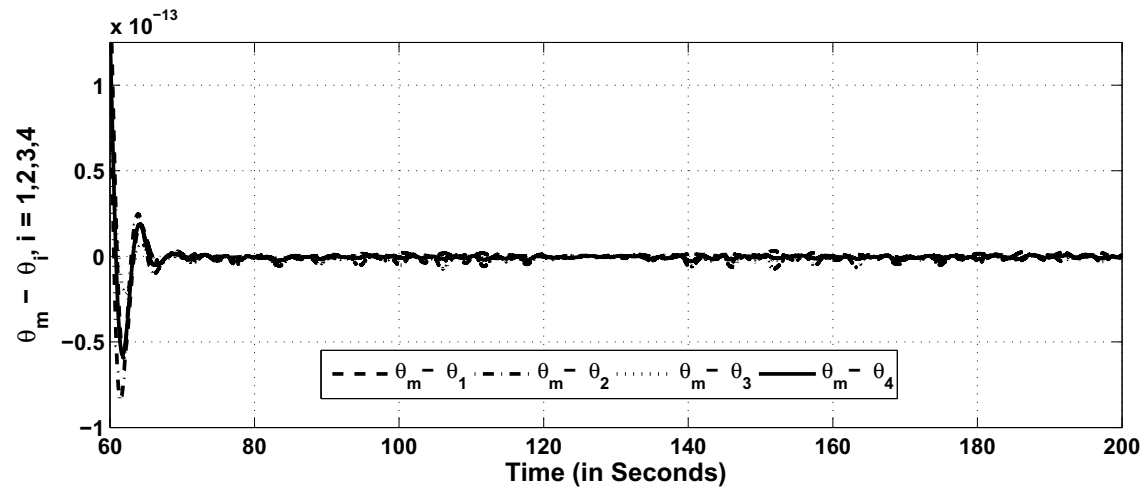


Figure 8

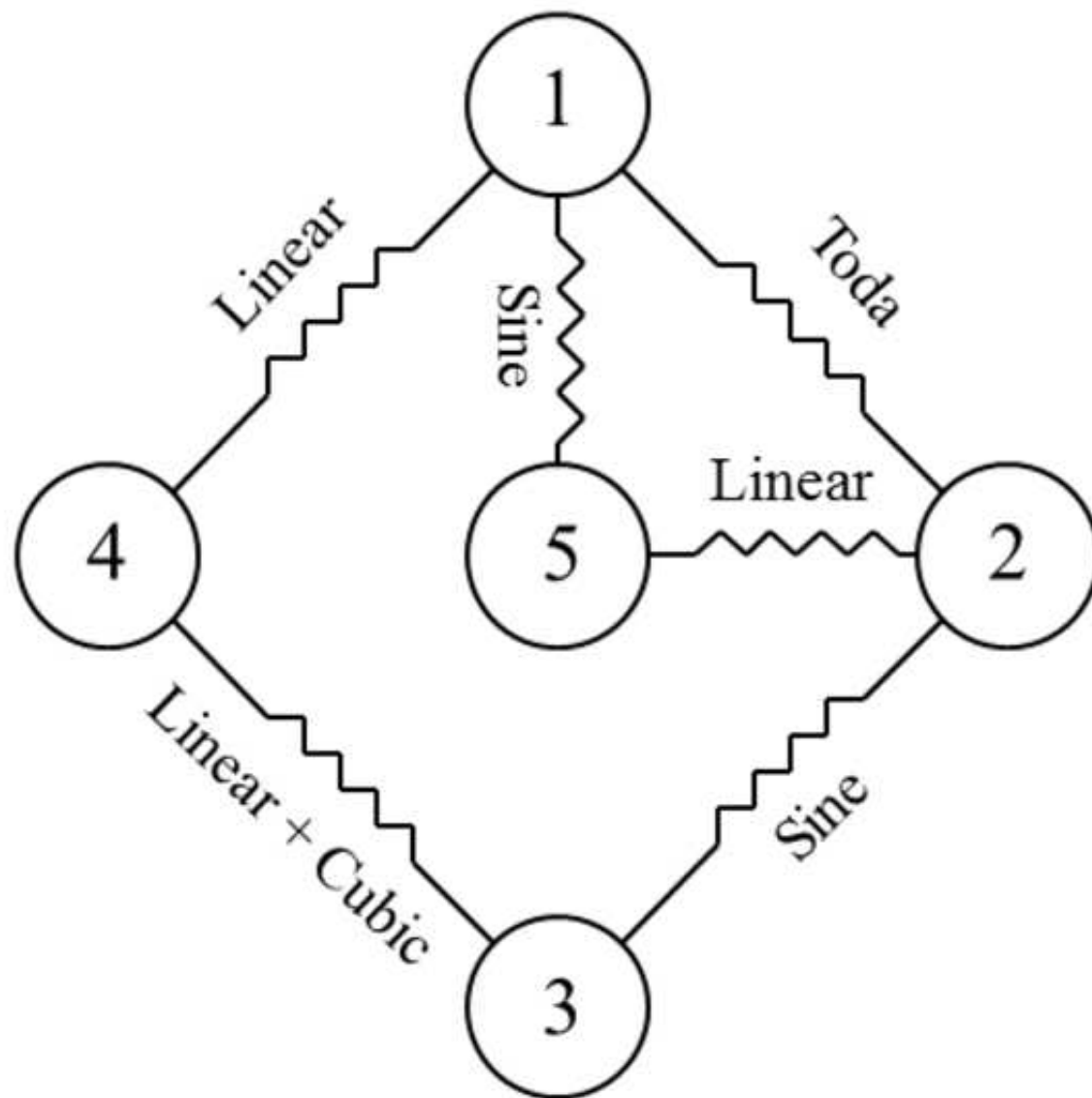
Journal of Aerospace Engineering. Submitted August 16, 2011; accepted December 14, 2011;  
posted ahead of print December 16, 2011. doi:10.1061/(ASCE)AS.1943-5525.0000192



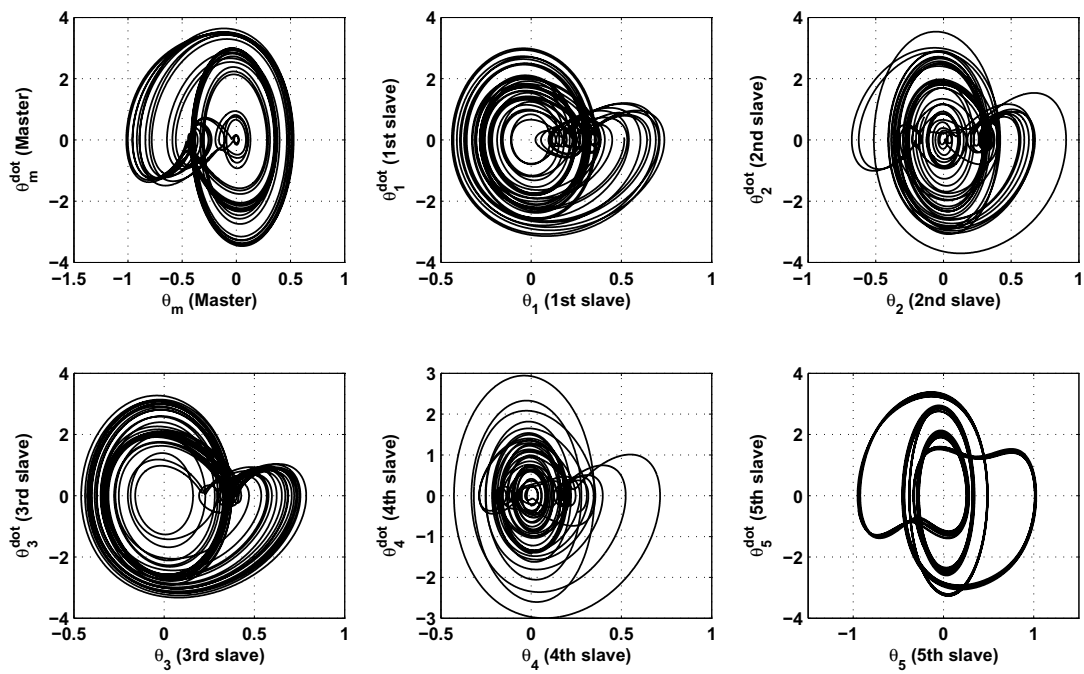
Accepted Manuscript  
Not Copyedited

Figure 9

Journal of Aerospace Engineering. Submitted August 16, 2011; accepted December 14, 2011;  
posted ahead of print December 16, 2011. doi:10.1061/(ASCE)AS.1943-5525.0000192



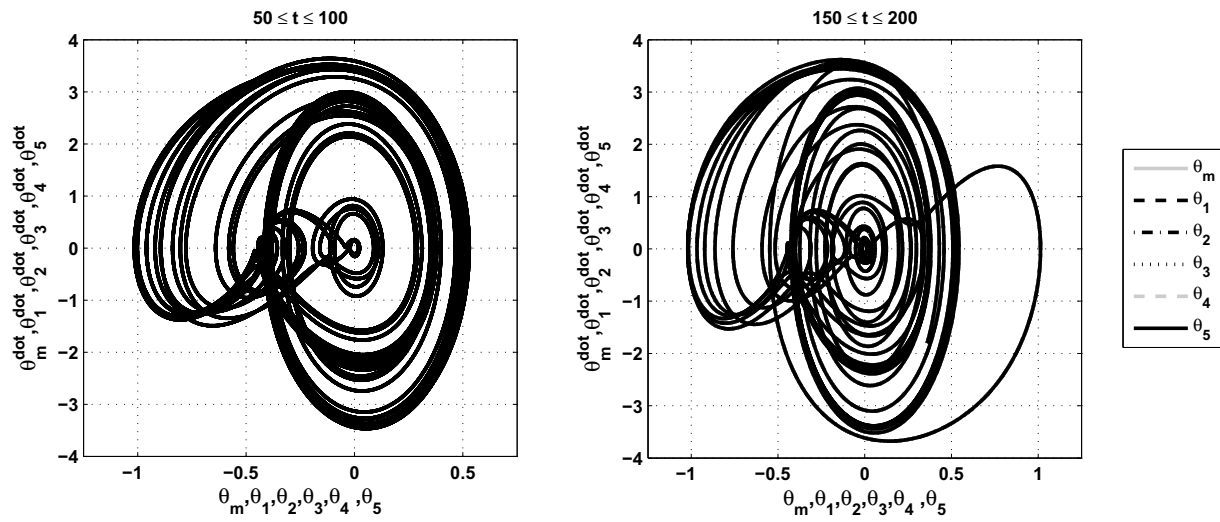
Accepted Manuscript  
Not Copyedited



Accepted Manuscript  
Not Copyedited

Figure 11

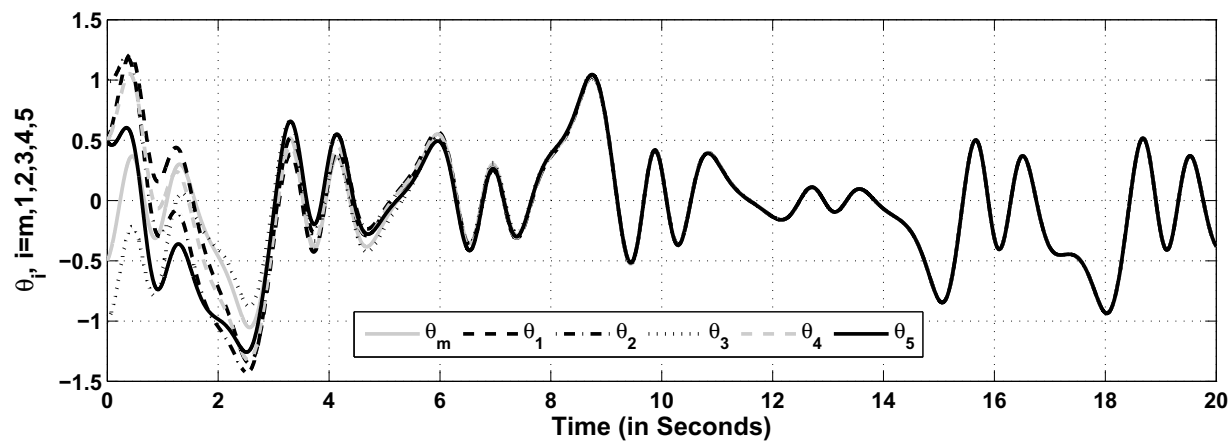
Journal of Aerospace Engineering. Submitted August 16, 2011; accepted December 14, 2011;  
posted ahead of print December 16, 2011. doi:10.1061/(ASCE)AS.1943-5525.0000192



Accepted Manuscript  
Not Copyedited

Figure 12

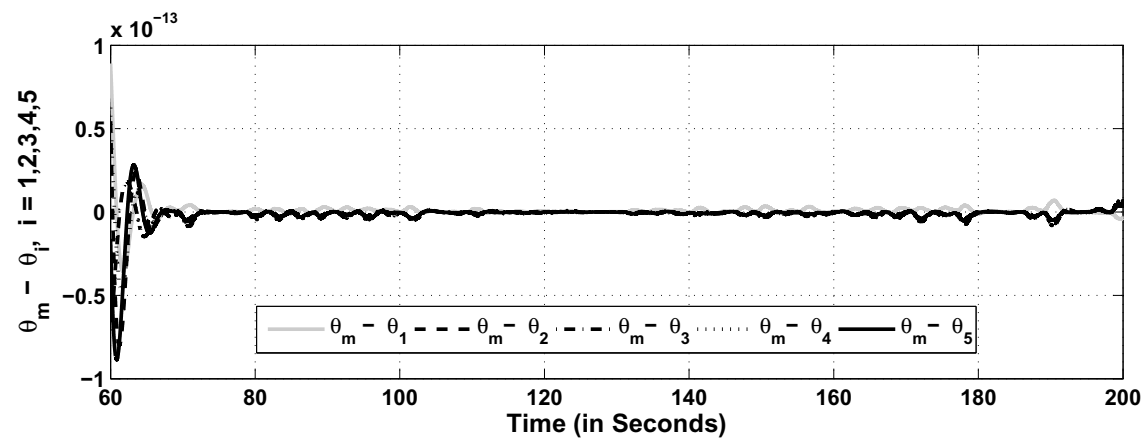
Journal of Aerospace Engineering. Submitted August 16, 2011; accepted December 14, 2011;  
posted ahead of print December 16, 2011. doi:10.1061/(ASCE)AS.1943-5525.0000192



Accepted Manuscript  
Not Copyedited

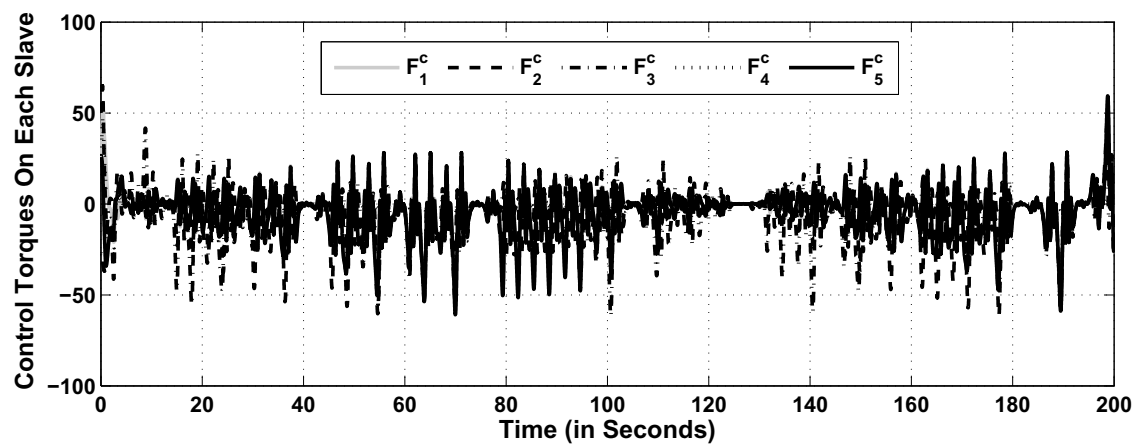
Figure 13

Journal of Aerospace Engineering. Submitted August 16, 2011; accepted December 14, 2011;  
posted ahead of print December 16, 2011. doi:10.1061/(ASCE)AS.1943-5525.0000192



Accepted Manuscript  
Not Copyedited

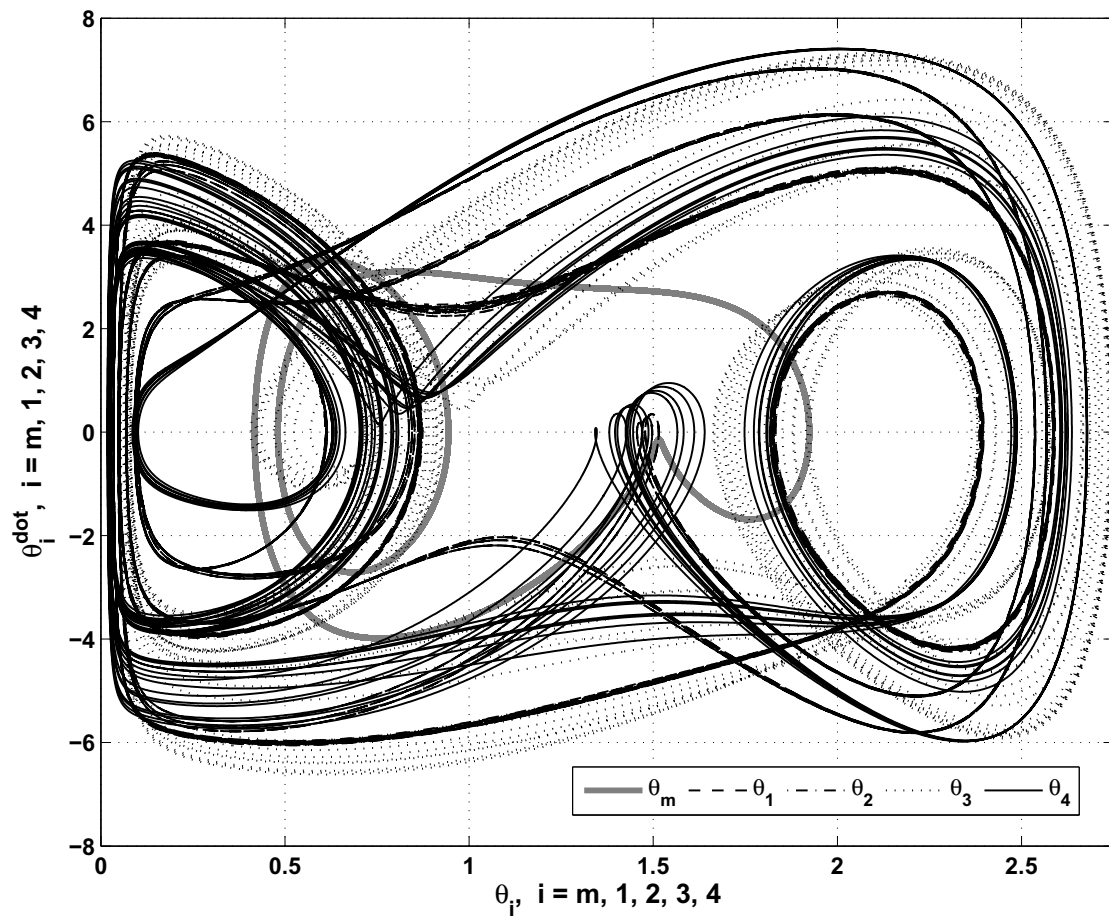
Journal of Aerospace Engineering. Submitted August 16, 2011; accepted December 14, 2011;  
posted ahead of print December 16, 2011. doi:10.1061/(ASCE)AS.1943-5525.0000192



Accepted Manuscript  
Not Copyedited

Figure 15

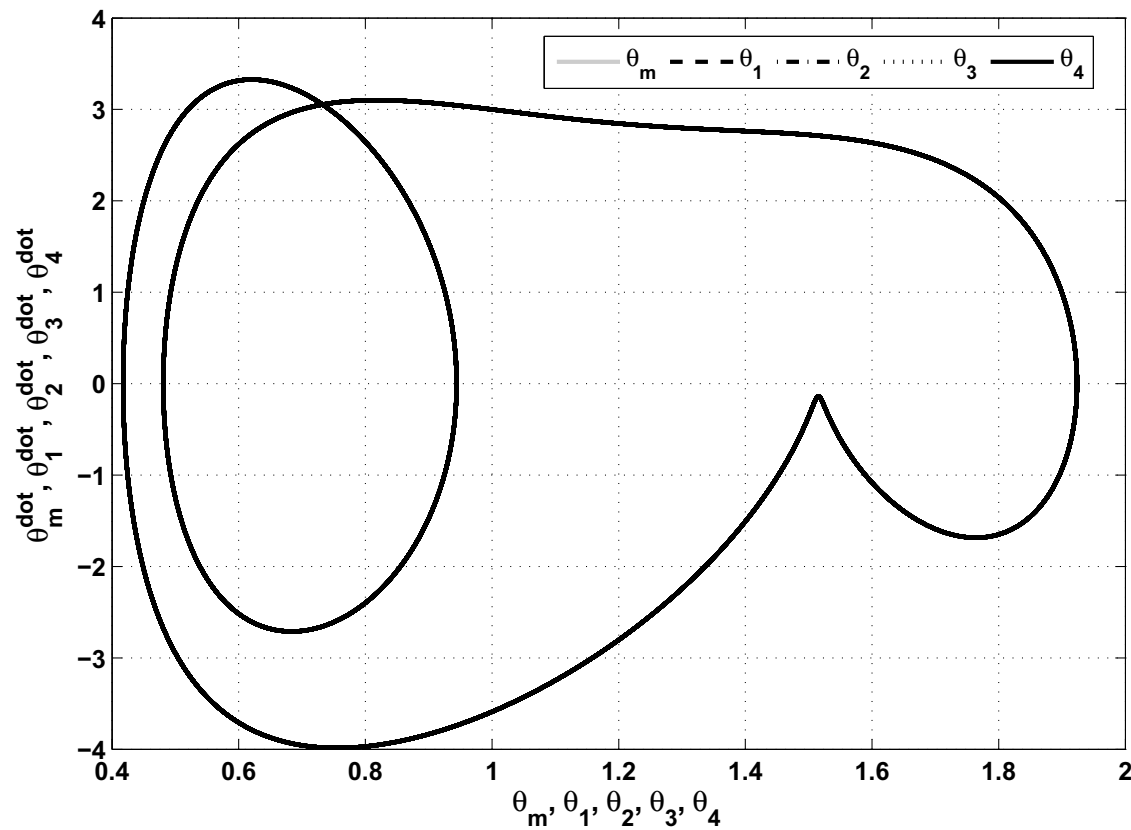
Journal of Aerospace Engineering. Submitted August 16, 2011; accepted December 14, 2011;  
posted ahead of print December 16, 2011. doi:10.1061/(ASCE)AS.1943-5525.0000192



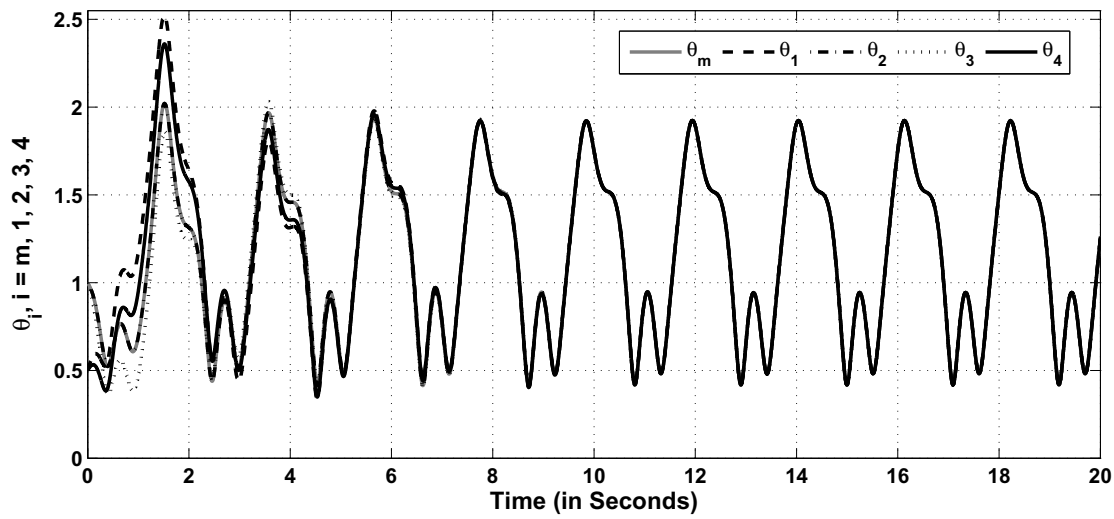
Accepted Manuscript  
Not Copyedited

Figure 16

Journal of Aerospace Engineering. Submitted August 16, 2011; accepted December 14, 2011;  
posted ahead of print December 16, 2011. doi:10.1061/(ASCE)AS.1943-5525.0000192

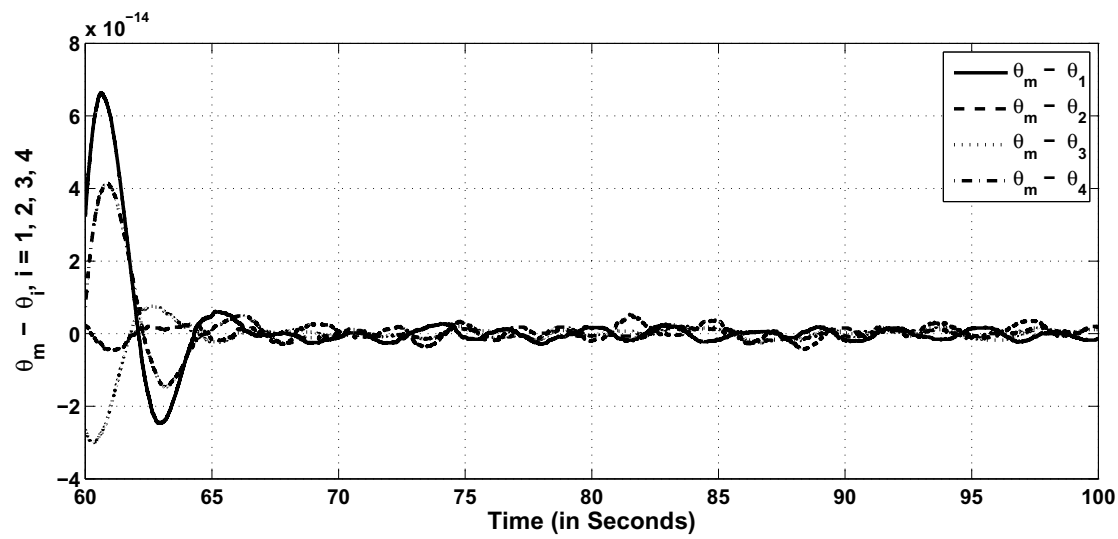


Accepted Manuscript  
Not Copyedited



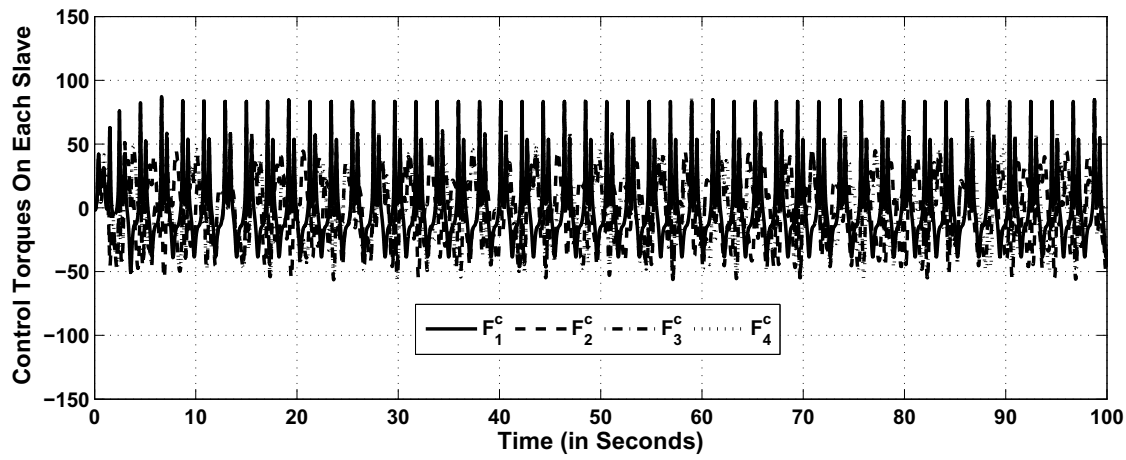
Accepted Manuscript  
Not Copyedited

Journal of Aerospace Engineering. Submitted August 16, 2011; accepted December 14, 2011;  
posted ahead of print December 16, 2011. doi:10.1061/(ASCE)AS.1943-5525.0000192



Accepted Manuscript  
Not Copyedited

Journal of Aerospace Engineering. Submitted August 16, 2011; accepted December 14, 2011;  
posted ahead of print December 16, 2011. doi:10.1061/(ASCE)AS.1943-5525.0000192



Accepted Manuscript  
Not Copyedited

Journal of Aerospace Engineering. Submitted August 16, 2011; accepted December 14, 2011;  
posted ahead of print December 16, 2011. doi:10.1061/(ASCE)AS.1943-5525.0000192

## Tables

<b>Name</b>	<b>Parameter Sets</b>	<b>Initial Conditions</b>
Master gyroscope (Periodic)	$P_m = [10.5, 1, 0.5, 0.02, 38.7, 2.2, 1]$	$IC_m = [-1, 0.5, 0]$
First Slave gyroscope	$P_1 = [10, 1, 0.5, 0.05, 35.5, 2, 1];$	$IC_1 = [0.5, 1, 0]$
Second Slave gyroscope	$P_2 = [10.5, 1, 0.5, 0.04, 38.5, 2.1, 2];$	$IC_2 = [1, -0.5, 0]$
Third Slave gyroscope	$P_3 = [10, 1, 0.5, 0.03, 35.8, 2.05, 1.5];$	$IC_3 = [-0.5, 1, 0]$
Fourth Slave gyroscope	$P_4 = [10.5, 1, 0.45, 0.045, 36, 2.05, 1.7];$	$IC_4 = [0.5, 0.5, 0]$

Table 1: Parameter and initial conditions sets for the five gyroscopes.

<b>Name</b>	<b>Parameter Sets</b>	<b>Initial Conditions</b>
Master gyro (Chaotic)	$P_m = [10, 1, 0.5, 0.03, 35.8, 2.05, 1]$	$IC_m = \{-0.5, 1, 0\}$
First gyro	$P_1 = [10, 1, 0.5, 0.05, 35.5, 2, 2]$	$IC_1 = \{0.5, 1, 0\}$
Second gyro	$P_2 = [10.5, 1, 0.5, 0.04, 38.5, 2.1, 1.3]$	$IC_2 = \{1, -0.5, 0\}$
Third gyro	$P_3 = [10.5, 1, 0.5, 0.02, 38.7, 2.2, 0.9]$	$IC_3 = \{-1, 0.5, 0\}$
Fourth gyro	$P_4 = [10.5, 1, 0.45, 0.045, 36, 2.05, 1.5]$	$IC_4 = \{0.5, 0.5, 0\}$
Fifth gyro	$P_5 = [10.5, 1, 0.5, 0.05, 38.5, 2, 1.7]$	$IC_5 = \{0.5, -1, 0\}$

Table 2: Parameter and initial condition sets for the six gyroscopes.

<b>Name</b>	<b>Parameter Sets</b>	<b>Initial Conditions</b>
Master gyro (Periodic)	$P_m = [2.5, 1.5, 0.45, 0.045, 35, 3, 1.5, 2.5]$	$IC_m = [1, -0.5, 0]$
First Slave gyro	$P_1 = [1.35, 1.1, 0.44, 0.044, 36.1, 3, 1.9, 2.1]$	$IC_1 = [0.5, 1, 0]$
Second Slave gyro	$P_2 = [1, 1.0, 0.44, 0.044, 35, 2.5, 2, 2.2]$	$IC_2 = [1, -0.5, 0]$
Third Slave gyro	$P_3 = [1.04, 1.0, 0.45, 0.045, 36.0, 2.06, 1.5, 1.8]$	$IC_3 = [1, -1, 0]$
Fourth Slave gyro	$P_4 = [1, 1.1, 0.45, 0.045, 36.0, 2.05, 2.05, 2.15]$	$IC_4 = [0.5, 0.5, 0]$

Table 3: Parameter and initial condition sets for the five gyroscopes.

Accepted Manuscript  
Not Copyedited